

Structured interactions as a stabilizing mechanism for competitive ecological communities

Violeta Calleja-Solanas,¹ Nagi Khalil,² Jesús Gómez-Gardeñes,^{3,4,5} Emilio Hernández-García,¹ and Sandro Meloni^{1,*}

¹*Institute for Cross-Disciplinary Physics and Complex Systems (IFISC), CSIC-UIB, 07122 Palma de Mallorca, Spain*

²*Complex Systems Group & GISC, Universidad Rey Juan Carlos, Móstoles 28933, Madrid, Spain*

³*GOTHAM Lab., Institute for Biocomputation and Physics of Complex Systems (BIFI), University of Zaragoza, 50018 Zaragoza, Spain*

⁴*Departamento de Física de la Materia Condensada, Universidad de Zaragoza, 50009 Zaragoza, Spain*

⁵*Center for Computational Social Science (CCSS), University of Kobe, Kobe (Japan)*

(Dated: October 4, 2022)

How large ecosystems can create and maintain the remarkable biodiversity we see in nature is probably one of the biggest open questions in science, attracting attention from different fields, from Theoretical Ecology to Mathematics and Physics. In this context, modeling the stable coexistence of species competing for limited resources is a particularly challenging task. From a mathematical point of view, coexistence in competitive dynamics can be achieved when dominance among species forms intransitive loops. However, these relationships usually lead to species' relative abundances neutrally cycling without converging to a stable equilibrium. Although in recent years several mechanisms have been proposed, models able to explain species coexistence in competitive communities are still limited. Here we identify locality in the interactions as one of the simplest mechanisms leading to stable species coexistence. We consider a simplified ecosystem where individuals of each species lay on a spatial network and interactions are possible only between nodes within a certain distance. Varying such distance allows to interpolate between local and global competition. Our results demonstrate, within the scope of our model, that species coexist reaching a stable equilibrium when two conditions are met: individuals are embedded in space and can only interact with other individuals within a short distance. On the contrary, when one of these ingredients is missing, large oscillations and neutral cycles emerge.

I. INTRODUCTION

The stability of ecosystems is a long-standing question in ecology [1–3]. Despite their complexity, ecological systems present remarkable biodiversity that persists for long periods of time. This fact has attracted large attention from several fields in the context of complex systems, in many cases bringing tools from statistical physics or the physics of disordered systems [4, 5]. Throughout the years, multiple mechanisms have been proposed to explain this persistence, including models based on random interactions [1] and niche theory [2, 6]. In particular for competitive communities, intransitivity [7–9] or higher-order interactions [10–13] have been identified as relevant ingredients to sustain biodiversity.

Most mathematical models for competitive communities establish a hierarchy among species, where the superior one will drive all the others to extinction, an effect called the competitive exclusion principle [14]. Despite of it, several mechanisms have been proposed to understand the multiplicity of species observed in natural systems. In particular, the absence of a dominant species can be explained if dominance among them is established as in a “Rock-Paper-Scissors” tournament, where species i out-competes j and j beats k , but k is superior to i , forming intransitive cycles. That is, intransitivity may play an important role in the promotion of species coexistence [7], while the structure of the dominance among species may shape their abundance [8]. Moreover, intransitive tournaments can be defined in probabilistic terms where one species out-competes the other with certain probability; allowing for endogenous stochasticity in the dynamics.

Concerning stability, the presence of large oscillations in populations is generally considered to be negative for biodiversity maintenance, since species can easily become extinct by external perturbations. Models implementing intransitive dominance often lead species abundances to neutrally cycle around an equilibrium point, something that is unlikely to occur in nature. To overcome this, one of the many approaches that have been proposed is the inclusion of so-called higher-order interactions – interactions in which the effect of one species on another is modulated by further species [11, 12]–leading to convergence to equilibrium, stabilizing the dynamics [10]. This and other approaches focus on interactions between species and ignore that, within species, single individuals can compete in diverse ways with multiple partners, whose identity can change in time and also in space (*i.e.* ignoring structured interactions).

However, spatial heterogeneity can also have an important impact on species coexistence [15–18]. The spatial arrangement of individuals can significantly affect the magnitude of their mutual influences, and hence the resulting dynamics. In the same way, the nature of ecological interactions may also shape the spatial distribution of individuals. Diverse works identify space as a driver of coexistence, but it is typically only intended to affect biotic or environmental rates [16, 18]. The spatial patterns that arise are determined by numerous controlling factors, which can be related to spatial disturbances [17], self-organization processes [19], early warning signals of ecological transitions [20] or space-dependent ecological interactions [16], also with intransitive competition [8]. Among the ecological processes that depend on spatial location, seed dispersal may have consequences in ecosystem's coexistence and diversity [21, 22]. However, even if the effect of spatial organization on species coexistence has been in the spotlight for years [9], the question of its role in the emergence and main-

* sandro@ifisc.uib-csic.es

tenance of stability in competitive intransitive communities, as a way to produce structured interactions, has not been fully explored.

Here, considering the competitive dynamics that arise from the spatial proximity between sessile individuals, we demonstrate that space has a stabilizing effect on competitive communities similar to that induced by higher-order interactions. As a starting point, we study simplified competitive dynamics where competition for resources takes place between pairs of individuals (pairwise interactions) and it is ruled by probabilistic intransitive cycles. We then explicitly introduce space into this framework by defining an interaction network between individuals. Its nodes represent single individuals of different species and links are drawn according to their distance. Positioning individuals in space limits competition to only adjacent neighbors, effectively reducing their mixing. Finally, varying the distance at which links are created allows us to interpolate between local and global interactions and study their effect on the dynamics. This representation provides a suitable context to test whether the spatial distribution of individuals, together with the range of competitive interactions, may be candidate mechanisms for the maintenance of biodiversity, as alternative to higher-order interactions.

Extensive numerical simulations of our model and of an analytical approximation of the system's dynamics prove that, when we consider only local competition, species abundances naturally converge to the equilibrium without the need of introducing other control mechanisms. These results are built on the fact that there is an underlying spatial structure and are not attainable by considering interactions of a given individual with just a small number of randomly chosen competitors. On the other side, when the range at which interactions occur increases, abundances start to oscillate in cycles of amplitude increasing with the interaction range. The stabilizing effect of space can be explained by analyzing spatial patterns formed by the species when interactions are local.

In Section II we define our model, and describe the results of its numerical simulations in Sect. III. We summarize our conclusions in Sect. IV. The paper is completed by two Appendices that contain some analytical approaches to the model.

II. COMPETITIVE COMMUNITY MODEL

We consider an isolated community with a fixed large number of individuals, N , each belonging to one of g different species, and model the effect of space in two ways. Firstly, space affects the arrangement of individuals; which we take into account within a network representation: each individual occupies a node, that symbolizes a fixed spatial location. A node only hosts one individual at a time. These locations can be regularly spaced or assigned at random. Secondly, two individuals compete if there is a link between them. Links are created according to the interaction range, where short ranges lead to local interactions between nearby nodes. Long-range interactions, instead, result in global competition and loss of spatial correlations.

A. Dynamical model

In order to focus on the interplay between space and stability, we keep the number of involved processes to the minimum. Only two ecological processes are present, namely: deaths with identical rate for all species and competition for the vacant location that an individual leaves when it dies. Under these assumptions, our model is suitable for communities of organisms that are permanently attached to one place, as plants. Hence, we describe the model and illustrate our findings through the example of plants competing in a forest. Each plant lives in a fertile region that becomes immediately available after its death. In that situation, two randomly selected individuals, among all the plants within the interaction range, compete for dispersing their seedlings. This is done via a dominance-matrix approach, as described below. Finally, the winner occupies the vacant node with a descendant of the same species (Figure 1a).

The probability that a seed of species i wins in a competition with species j , H_{ij} , is encoded in the $g \times g$ dominance matrix H . The values of H_{ij} for $i > j$ are drawn uniformly at random, and we then set $H_{ji} = 1 - H_{ij}$, and $H_{ii} = 0.5$. Within this setting, the system reaches coexistence when H presents intransitive dominance cycles (that occur when $H_{ij} > H_{jk} > H_{ki} > 0.5$ for some triad i, j, k), in accordance with [10, 23]. Specifically, and for sake of reproducibility, in our numerical simulations we employ the following matrix:

$$H = \begin{pmatrix} 0.5 & 0.34 & 0.76 \\ 0.66 & 0.5 & 0.25 \\ 0.24 & 0.75 & 0.5 \end{pmatrix}. \quad (1)$$

Moreover, given the form of H , the ecosystem is constrained in the long-term to have an odd number of species [10]. When one species vanishes, another extinction event must occur to maintain the odd number of species.

B. Interactions' structure

To explore the effect of spatial arrangement, we employ three different types of networks: a 2D square lattice, a Random Geometric Graph [24] and an Erdős-Rényi graph [25]. Each network defines a certain type of spatial distribution.

A *2D square lattice* is our baseline for a highly-ordered space because of its simplicity and wide use in ecology [16, 17, 26]. Nodes are regularly distributed on the unit square and are at a discrete, constant distance apart from each other. The nearest neighbors of a node are considered to be the eight adjacent nodes (with periodic boundary conditions) (Figure 1b). This network, since nodes are regularly spaced and connected, can generate strong spatial correlations.

In addition to lattices, we consider a *Random Geometric Graph* (RGG) that conserves the spatial structure but in a disordered manner, as the N nodes are uniformly distributed in the unit square and two of them are linked if their Euclidean distance is smaller or equal to a particular interaction range

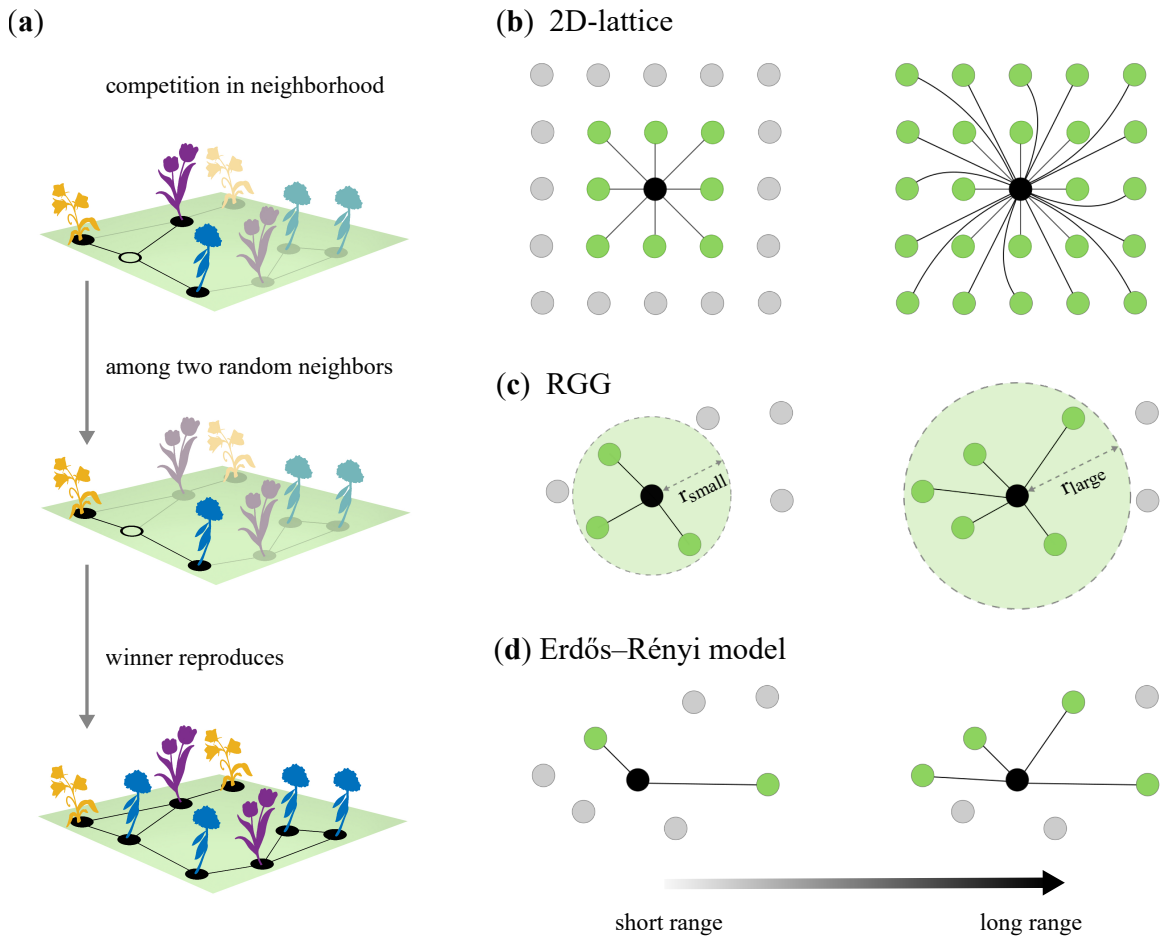


FIG. 1. Schematic representation of the interaction networks and competitive dynamics. (Panel a) Diagram of the model. A random plant is selected to die with a probability $1/N$, leaving a vacant fertile region (i.e. an empty node). Two (highlighted in the middle panel) of the three neighbors are selected at random. Finally, the winner is chosen according to the probabilities of the species dominance matrix H , and its descendant sprouts in the vacant node. (Panels b-d) Illustration of the three spatial interaction networks considered. The neighborhood of the black node is depicted (in green) for different interaction ranges. (Panel b) A 2D-lattice with a regular distribution of individuals. The left side of the panel depicts the neighborhood for the smallest possible interaction range while the right side highlights the neighborhood when the smallest interaction range has been increased by one unit. (Panel c) In a Random Geometric Graph, the coordinates of the individuals are uniformly set at random in the unit square and two nodes are connected if their Euclidean distance is less or equal than $R_{RGG} = r_{small}$ (left side of the panel) or $R_{RGG} = r_{large}$ (right side of the panel). (Panel d) Erdős-Rényi graphs have no spatial structure. Each pair of nodes connects with probability p independently of their distance. The left and right sides of the panel illustrate the same spatial arrangement as in Panel c, but the neighbors of the black node are determined at random by the linking probabilities $p = 0.2$ and $p = 0.4$ respectively.

R_{RGG} (Figure 1c) allowing us to study continuous distances and variability in the number of neighbors [27–29].

Finally, we consider non-spatial interactions through *Erdős-Rényi graphs* (ER), where nodes are connected at random with probability p and, hence, the location of individuals does not affect their linking probability (Figure 1d). In this case, spatial correlations are completely destroyed, although each node still has a finite number of neighbors.

Summing up, the ER graph is our null model since it has no spatial structure, while we include the RGG as a compromise between unstructured and regularly-spaced interactions.

We tune the competition from local to global in the different networks by means of the interaction range. This range

determines the individuals that participate in the competition, *i.e.* who interacts with whom. With short-range interactions, only nearby nodes compete. As it increases, more distant nodes enter the competition until the neighborhood size is large enough to dissolve the effect of location and consider the system well-mixed. In particular, for square lattices, this leads to connections between not only the closest nodes but also the second, the third groups of neighbors, etc. Meanwhile, increasing the interaction range in a RGG means increasing the distance R_{RGG} . Finally, position or distances between nodes do not enter into the construction of ER networks. In this case, the connection probability p serves as a proxy for the interaction range. Increasing p generates larger neighborhoods, all-

beit their location is at random. In order to use a quantity that can be compared with the other networks, it is convenient to quantify the interaction range by the mean degree $\langle k \rangle = pN$. For every network, we trivially get all-to-all competition with the largest interaction range.

III. RESULTS

Once our model has been defined, we start analyzing it through extensive Monte Carlo simulations. At the beginning of each simulation, the species within each node is assigned at random with a uniform probability $1/g$. We simulate the system using an asynchronous update scheme, where a generation is defined as N updates to ensure that, on average, every node has experienced a death event. Finally, we keep track of the proportion or relative abundance of individuals of each species in the system, $x_i(t) \equiv N^{-1} \sum_{\nu} n_{i,\nu}$, where $n_{i,\nu}$ takes the value 1 if and only if species i is present at node ν . Each node can host only one individual of a single species, which implies that $\sum_i n_{i,\nu} = 1, \forall \nu$. Since the total number of nodes in the system is constant and equal to the total number of individuals N , the macroscopic quantities x_i are also average total spatial densities.

Since we have $\sum_i^g x_i(t) = 1$ for every generation t , the relative abundances of all species can be represented by a point in the $(g-1)$ -simplex $\{(x_1, \dots, x_g) | x_i \geq 0 \text{ and } \sum_{i=1}^g x_i = 1\}$, whose vertices correspond to single-species populations. As time evolves, the point follows a trajectory on the simplex that characterizes the macroscopic state of the system.

A. Temporal evolution

We begin our analysis by inspecting the temporal evolution of species' abundances in the simplest situation of three competing species, $g = 3$. Unless otherwise stated, we use always the same matrix H given in Eq. (1), which gives results representative of any other randomly generated dominance matrix with intransitive cycles. We find different behaviors depending on the spatial distribution of species and the distance at which they interact. Species in communities with no spatial structure (all-to-all interactions, Figure 2a; same result for ER graphs) cycle on the simplex. The same wide oscillations (Figure 2b) can also be seen if we consider long-range interactions in structured communities (RGG and 2D-lattice). This first result is in line with the prediction of the mean-field approximation (see Appendix A). However, the amplitude of the observed oscillations is independent of the initial conditions, indicating that these oscillations are of the limit-cycle type, qualitatively different from the neutral ones predicted by the mean-field theory.

For the two spatial networks considered, decreasing the interaction range leads to a reduction in the amplitude of the oscillations until, for a sufficiently short-range, species' abundances only slightly fluctuate around an equilibrium state (Figure 2c).

Their value at this point is, in all cases analyzed, close to the equilibrium fixed point obtained from the mean-field approximation (which for the matrix H in Eq. (1) is $(x_1, x_2, x_3) = (0.374, 0.383, 0.243)$). These values also coincide with the temporal average of the relative abundances in the oscillatory case for the same matrix H .

These latter results reveal a non-trivial dependency of the dynamics on the interaction range, and demand a deeper analysis. For this purpose, in the next sub-sections, we systematically study the effect of the interaction range and structure on species' dynamics.

B. Dynamical behavior depends on structured interactions

As a first step, we need a measure to characterize the behavior of the system for each structure and interaction range. Because of the noisy character of the dynamics in the stochastic simulations, the amplitude of the oscillations is not a robust indicator. Instead, we consider the area encircled by the system's trajectory on the simplex. If the system fluctuates with small amplitude around some equilibrium abundances, the trajectory occupies a small area (Figure 2f), whereas larger oscillations would cover broader areas (Figure 2d,e).

Once defined our metric to characterize the stability of the dynamics, we can study the effect of space by keeping H fixed in all the simulations and varying the underlying network structure (the type of graph) and the interaction range. Since we cannot properly define distances in ER graphs, we use the degree as a proxy of interaction range for that graph. This equivalence can be made as the interaction range not only defines the distance at which nodes compete but also their degree. In that way, we are ready to compare the two spatial networks with the ER graphs.

To start with, we focus on the effect of the interaction network but without any spatial arrangement by considering the ER graphs with increasing average degree: *i.e.* increasing p (blue points in Figure 3). We find that the dynamics show large oscillations for all values of the degree. That is, the size of the neighborhood does not affect the dynamics.

However, this picture drastically changes when we consider spatially structured interactions.

We recover the results of the ER networks for large ranges (large average degrees) in both the RGG and the 2D lattice. However, the system stabilizes around the equilibrium point when we decrease the interaction range, covering a tiny area in the phase space. The transition between these two regimes takes place when the average degree of both networks is within the range $50 \lesssim \langle k \rangle \lesssim 100$.

To summarize, the intuitive picture that arises from these results is the following: when we consider long-range interactions – e.g. large degrees – we obtain large oscillations, which are similar to the ones obtained for non-spatial networks (ER). In all cases, the amplitude and period of the oscillations are independent of the initial conditions, *i.e.* the oscillations are of the limit-cycle type. The mean-field approximation (see Appendix A), which is expected to be valid in the limit of long-range interaction, correctly predicts oscillatory behavior.

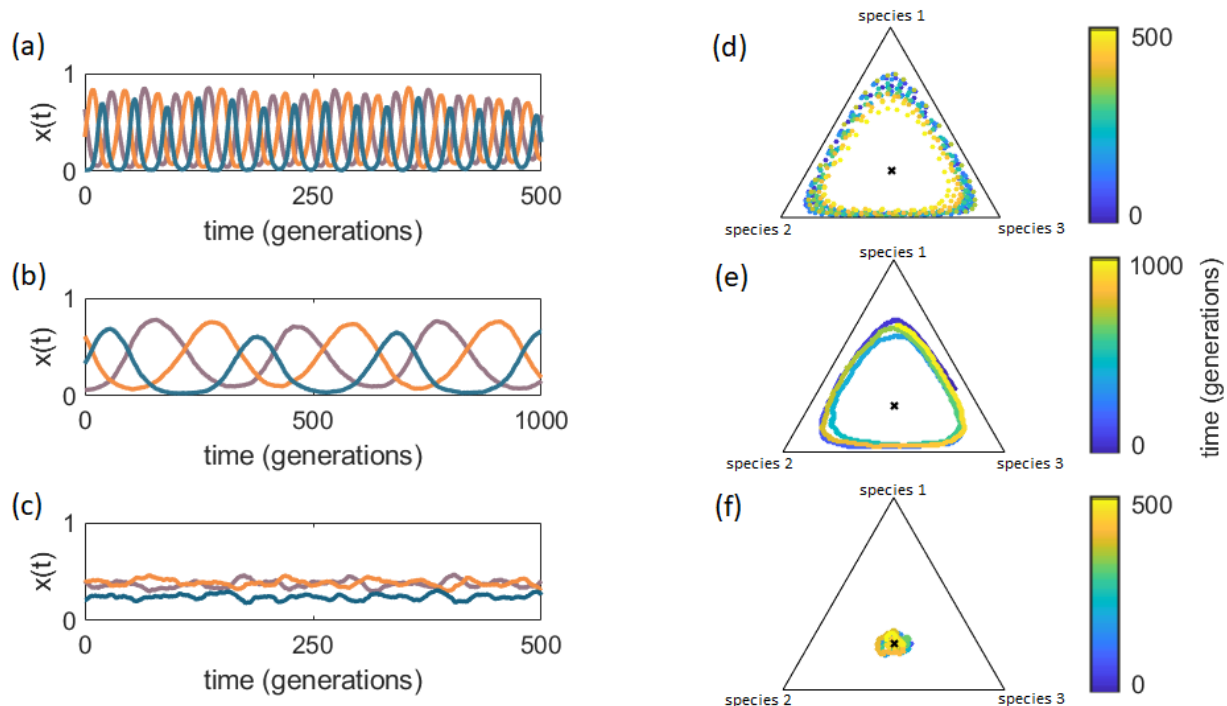


FIG. 2. (Panels a,b,c) Temporal evolution of the species relative abundances for a 3-species system, comparing different interaction schemes. In each panel, the ecosystem is represented by a RGG of $N = 10^4$ nodes. Relative abundances x_1, x_2, x_3 are plotted after the transient has vanished. (Panel a) All-to-all interactions: the range is set to cover the entire plane ($R_{RRG} = R_{max} = \sqrt{2}$), hence individuals can compete for any vacant node. (Panel b) Long-range interactions: we set $R_{RRG} = 0.15$ leading to an average degree $\langle k \rangle \simeq 706$. (Panel c) Short-range interaction: $R_{RRG} = 0.03$ and $\langle k \rangle \simeq 28$. (Panels d,e,f) Trajectories in the phase space represented on the standard 2-simplex (the portion of the $x_1 + x_2 + x_3 = 1$ plane in which $x_1, x_2, x_3 \geq 0$). The plots show a view perpendicular to the simplex, and correspond to the time evolution of the left panels. The color code represents time evolution. With all-to-all and long-range interactions (Panels d and e), abundances oscillate in large cycles around what seems to be an equilibrium point (represented by a black cross). With short-range interactions (Panel f), abundances remain confined in a small region around the equilibrium.

But it fails to reproduce the limit-cycle character, predicting neutral oscillations instead. When we restrict competition to small neighborhoods (small degrees) we find that the dynamics stabilizes around some fixed point x^* .

C. Spatial configurations

So far we have only considered the trends of the global relative abundances, x_i , quantities that are influenced by, but do not explicitly display information on, the spatial distribution of individuals. To better understand the mechanism behind the reported behavior, we show in Figure 4 two different snapshots of the spatial organization of a 3-species system in a 2D square lattice for two different interaction ranges (short and long).

With short ranges (Figure 4a), species self-organize in mono-specific patches. Changes in species relative abundances can only take place along the borders, where different species meet. A death event inside the patch does not contribute to relative abundance variations because competition is among same-species individuals. In this way, patches are

more robust to invasion from other species, decelerating the dynamics of the system and hence the possibility of heavy oscillations.

Differently, with long-range interactions (Figure 4b), the unstructured and statistically homogeneous solution predicted by mean-field theory appears: vacant nodes can be reached by any species blocking the formation of single-species clusters. The absence of patches prevents the community from reaching a steady state, with intransitive cycles generating large-scale oscillations.

Taken together, these latter results suggest that short-range interactions reduce the effective competition in the system by decreasing the probability of an encounter between individuals of different species. To confirm this hypothesis, we calculate the average probability $\langle P_{ij} \rangle$ that two species i and j compete for a vacant node in the short-range regime and compare it with the expected value \bar{P}_{ij} in the all-to-all case. $\langle P_{ij} \rangle$ has been obtained numerically by recording the number of times species i and j have been selected for competition and then averaging over the duration of the simulation. For all-to-all interactions, \bar{P}_{ij} is given by the product of the relative abundances of species i and j at the mean-field equilibrium

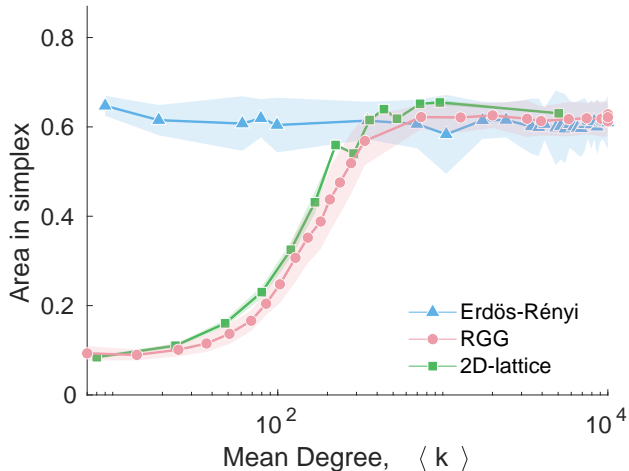


FIG. 3. Average area inside the trajectory on the 2-simplex of the (x_1, x_2, x_3) point of a 3-species community (see Figure 2, Panels d-f) as a function of average degree $\langle k \rangle$, for different networks. The total number of individuals is $N = 10^4$, and the same dominance matrix H is used for all networks. The points represent the mean area obtained over 50 realizations, each simulated in different networks. Areas have been calculated excluding the 5% of out-layer points in the trajectory. Shaded areas indicate 95% confidence interval.

abundances $\bar{P}_{ij} = x_i^* x_j^*$ (see Appendix A). For our example system we have $x^* = (0.374, 0.383, 0.243)$, so that:

$$\bar{P}_{ij} = \begin{pmatrix} 0.1399 & 0.1432 & 0.0909 \\ 0.1432 & 0.1467 & 0.0931 \\ 0.0909 & 0.0931 & 0.0590 \end{pmatrix} \quad (2)$$

The computation of matrix $\langle P_{ij} \rangle$ for Eq. (1), in a RGG with short-range interactions ($R_{RGG} = 0.022$ and $\langle k \rangle \simeq 15$) gives the following result:

$$\langle P_{ij} \rangle = \begin{pmatrix} \mathbf{0.2160} & 0.0965 & 0.0597 \\ 0.0965 & \mathbf{0.2241} & 0.0659 \\ 0.0597 & 0.0659 & \mathbf{0.1156} \end{pmatrix}. \quad (3)$$

We see that, when compared to the all-to-all case, for short-range interactions, same-species competition has a higher probability to occur ($\langle P_{ii} \rangle$, highlighted in boldface in Eq. (3)) than different-species competition (the off-diagonal terms). This demonstrates that spatial inhomogeneities reduce the effective inter-specific competition. Finally, as a further confirmation of this mechanism, in Appendix B we show that a toy model, based on the mean-field formulation of the model but where inter-specific interactions are reduced and intra-specific ones are increased, presents the same shift in stability observed in our spatial models.

D. Stability and fluctuations

Once clarified the mechanism behind the stabilization of the dynamics for short interaction ranges, we conclude our

analysis by probing further the stability of the fixed point for the macroscopic variables x_i , and by studying the nature of the fluctuations around it that are seen in the simulations.

To check the stability of the equilibrium reached, we study the system's response to pulse perturbations of different magnitudes. In our model, this translates into imposing a sudden change in species' relative abundances and measuring the time needed to recover the original state. Figure 5a shows the results for a RGG for $R_{RGG} = 0.03$ (short range), with a 90% perturbation of one species' relative abundance (with all other abundances being proportionally decreased), demonstrating that, even with such a large disruption, the dynamics bounce back to the equilibrium as the perturbation decays exponentially in time.

Finally, we study the characteristics of the fluctuations around the equilibrium for both the stable and the unstable regimes. To do so, we focus on how the size of fluctuations in the relative abundance of each species (defined as their coefficient of variation, $\sigma_i / \langle x_i \rangle$) scales with the size of the system. In Figure 5b we show the scaling for one species in a RGG. For small degrees ($\langle k \rangle = 15 \pm 2$), we find an exponent of 0.47, pretty close to the 0.5 expected in case of residual fluctuations arising from many nearly uncorrelated domains and the stochastic noise due to the finite size of the system. This rules out the possibility that the observed fluctuations originate from the presence of oscillatory behavior of small amplitude. In turn, for the unstable case (large degrees, $\langle k \rangle = 980 \pm 190$) we observe an exponent of 0.14. In this case, fluctuations are a genuine ecological signal that emerges from the interactions in a high-mixing environment.

IV. DISCUSSION AND CONCLUSIONS

Many efforts have been made to explain the remarkable robustness observed by natural ecosystems in terms of biodiversity. These efforts include niche and neutral models and higher-order interactions. Here, considering a minimal model for competitive communities, we have proved that spatial interactions alone lead to the coexistence and stability of multi-species systems.

In particular, making use of extensive numerical simulations we have studied a simple model where multiple species compete in a structured space in intransitive dominance cycles. Analyzing different spatial arrangements, ranging from regular lattices to random connections that cancel out the effect of space, our results show that spatial interactions limited to nearest neighbors lead to stable coexistence of different species, while for long-range interactions species' relative abundances indefinitely oscillate. By taking into account the spatial organization of the individuals, we discovered that local interactions allow species to survive by forming mono-specific patches where competition only takes place at their borders and, as result, decreasing the effective competition experienced by each individual. This latter effect generates a deceleration of the dynamics, effectively damping out fluctuations. These last results, however, are not matched by mean-field approximations, as described in Appendix A. This is not

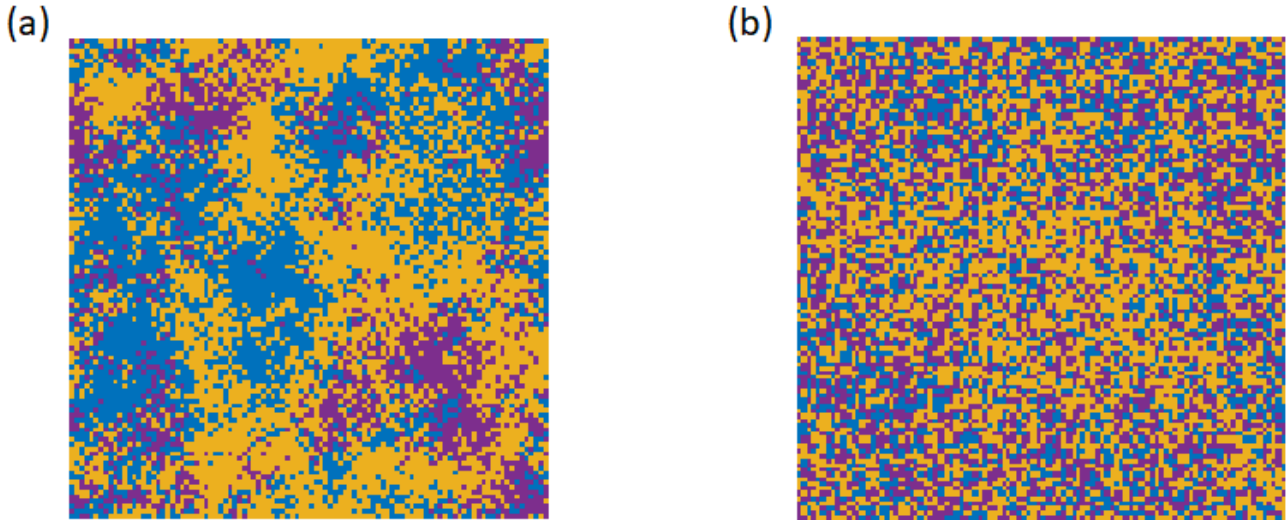


FIG. 4. Spatial organization of a 3-species community in a 2D-lattice of $N = 10^4$ for short and long-range interactions with the dominance matrix given in Eq. (1). Individuals of each species are depicted in a different color. (Panel a) Short-range interactions: when a plant dies only the 8 closest neighbors at distance one compete for a vacant node (see the left network from Figure 1b). (Panel b) Long-range interactions: the 360 individuals at distance less or equal to 9 from a vacant node participate in the competition.

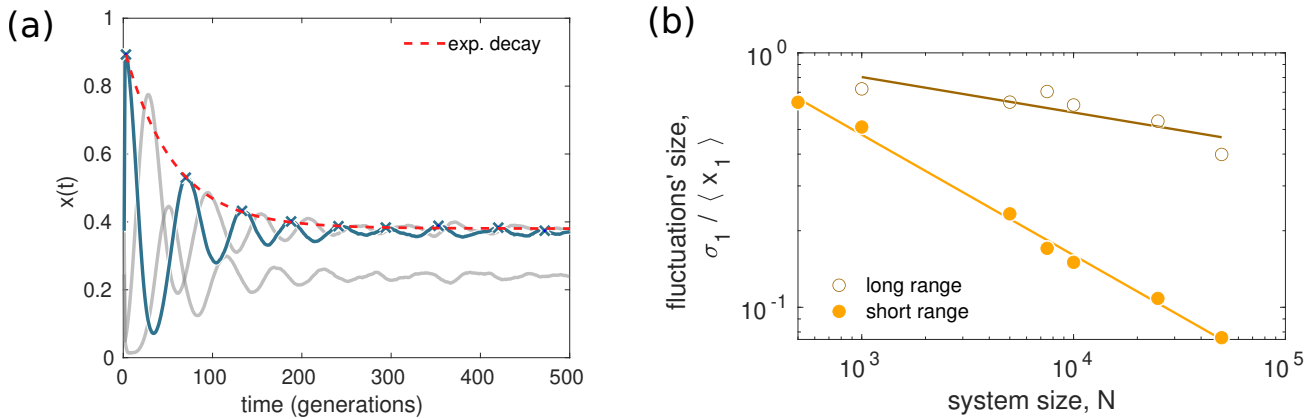


FIG. 5. (Panel a) Time evolution of the recovery from a 90% pulse perturbation in a 3-species community for the dominance matrix H of Eq. (1). The relative abundance of one species (blue) is artificially modified from its equilibrium value to be the 90% of the whole population, whereas other species' relative abundances (in grey) are proportionally decreased. The simulation is performed in a RGG of 10^4 individuals and $R_{RGG} = 0.03$. The red line represents the fit of the local maxima of the relative abundance (blue crosses) to the function $ae^{-\alpha} + b$ with $\alpha = 0.018$, $a = 0.53$ and $b = 0.38$. (Panel b) Scaling of fluctuations, measured by the coefficient of variation of species 1 ($\sigma_1 / \langle x_1 \rangle$) with the system size N for a RGG with 3 species. Each point is the result of 10 different realizations where the variance and mean relative abundance of species 1 have been calculated over at least $\Delta t = 10^8$ time-steps after the transient. Short-range interactions correspond to an average degree $\langle k \rangle = 15 \pm 2$, and we find a decrease of the relative fluctuations with system size as $\sigma_1 / \langle x_1 \rangle \sim N^{-0.47}$, consistent with an scenario of uncorrelated domains. For a situation of long-range interactions we set $\langle k \rangle = 980 \pm 190$, giving a scaling of the relative fluctuations as $N^{-0.14}$.

surprising since the dynamics depend strongly on the nature of the spatial correlations created by the finite-range interactions.

In conclusion, even if our results are obtained with a simplified model, taken together our findings help to explain the role of space in maintaining stable spatial coexistence in natural ecosystems. In this sense, a restricted interaction range goes

against the coherent and neutral oscillatory behavior usually produced by intransitive interactions. While in real ecosystems many simultaneous mechanisms may be at play, as for example higher-order interactions, spatial effects are probably the simplest and most widely present of them, and thus they need to be considered when addressing ecological coexistence.

ACKNOWLEDGMENTS

V.C-S. and S.M. thank Hugo Saiz for insightful discussions. J.G.G. acknowledges support by Gobierno de Aragon/Fondo Social Europeo (E36_20R FENOL group), grant FIS2017-87519-P funded by Spanish MINECO, and grant PID2020-113582GB-I00 funded by MCIN/AEI/10.13039/501100011033.E.H-G., S.M. and V.C-S. acknowledge the Spanish State Research Agency, through the Severo Ochoa and María de Maeztu Program for Centers and Units of Excellence in R&D (MDM-2017-0711) funded by MCIN/AEI/10.13039/501100011033. V.C-S. acknowledges support from FPI/2257/2019 Conv. 201, CAIB PhD program. N.K. acknowledges support by Rey Juan Carlos University (Grant M2605) and by Community of Madrid and Rey Juan Carlos University through Young Researchers program in R&D (Grant CCASSE M2737).

Appendix A: Analytical formulation

Along with a numerical implementation of the dynamics, it is also possible to provide a mathematical description of the model, which we set up in this Appendix. In Section A 1 we establish the basic equations for the moments of the population variables. Sect. A 2 develops a standard mean-field approximation for statistically homogeneous systems. We stress that it is not able to reproduce the main numerical findings for our model, but gives a baseline to interpret the results. Sect. A 3 extends the mean-field approximation to allow for spatial inhomogeneity in the species distribution. The results still do not match with the numerical observations, but give some hints on the reduced stability of homogeneous oscillations when the interaction range is small.

1. Moment equations

An analytical description of the stochastic dynamics defined in the main text can be given (after a trivial replacement of the discrete-time dynamics by a continuous-time one) by the master equation for the time-dependent probability of the system state. It allows us to derive equations for the expected relative abundance of each species at a given node as well as for the two-node correlations.

The model state can be specified by giving $\{Z_\nu\}$, where $Z_\nu = 1, 2, \dots, g$ specifies the species that occupies node $\nu \in \Sigma$, with Σ being the set of nodes of the network. However, we find more convenient to parameterize the model as follows. Let $n_{i,\nu} \in \{0, 1\}$ be the number of individuals of species $i \in \{1, \dots, g\}$ at node $\nu \in \Sigma$, i.e. $n_{i,\nu} = 1$ for one and only one i , identifying the species present at ν , and 0 for the other values of i (absent species). The state of the system can be characterized by the set of vectors $S = \{S_\nu\}_{\nu=1}^N$, with $S_\nu = \{n_{1,\nu}, \dots, n_{g,\nu}\}$. This state evolves as follows: (i) with a rate r , a randomly chosen individual (say, located at ν) dies, then (ii) two neighbors of the dead individual (thus pertaining

to the set P_ν of neighbors of ν) are chosen at random and compete to generate the offspring: a winner species is selected according to the probabilities in the dominance matrix H . And (iii) this offspring is immediately located at the vacant node. Following standard procedures (for example see [30, 31]) the master equation for the probability $p(S, t)$ of finding the system in a state S at time t can be written as

$$\frac{\partial}{\partial t} p(S, t) = \sum_{\nu=1}^N \sum_{i,j} (E_{i,\nu}^+ E_{j,\nu}^- - 1) \pi_\nu(i \rightarrow j) p(S, t), \quad (\text{A1})$$

where the operators E^\pm act on an arbitrary state function $f(S)$ as

$$E_{i,\nu}^\pm f(S) = f\left(\{n_{1,1}, \dots, n_{g,1}\}, \dots, \{n_{1,\nu}, \dots, n_{i,\nu} \pm 1, \dots, n_{g,\nu}\}, \dots, \{n_{1,N}, \dots, n_{g,N}\}\right). \quad (\text{A2})$$

$\pi_\nu(i \rightarrow j)$ is the rate at which an individual of species i is replaced by one of species j at site ν , given by

$$\pi_\nu(i \rightarrow j) = r \frac{n_{i,\nu}}{N} \frac{2}{k_\nu(k_\nu - 1)} \sum_{\substack{\lambda, \mu \in P_\nu \\ \mu \neq \lambda}} \sum_k n_{j,\lambda} n_{k,\mu} H_{jk}, \quad (\text{A3})$$

where k_ν is the degree of node ν , i.e. the number of nodes in P_ν .

From the master equation we can derive equations for the moments of the distribution, which can be easily measured from the numerical simulations. The simplest nontrivial moment is the expected number of individuals of species i at node ν , $\langle n_{i,\nu} \rangle$. Its equation is readily obtained from the master equation after multiplying it by $n_{i,\nu}$ and summing over all possible values of S :

$$\frac{d}{ds} \langle n_{i,\nu} \rangle = \frac{1}{k_\nu(k_\nu - 1)} \sum_j \sum_{\substack{\lambda, \mu \in P_\nu \\ \mu \neq \lambda}} H_{ij} \langle n_{i,\lambda} n_{j,\mu} \rangle - \frac{1}{2} \langle n_{i,\nu} \rangle, \quad (\text{A4})$$

where we have introduced a new time scale $s \equiv \frac{2r}{N} t$.

From this equation we can write the dynamics for the expected value of the macroscopic variable $x_i(s) \equiv N^{-1} \sum_\nu n_{i,\nu}$ as

$$\frac{d}{ds} \langle x_i(s) \rangle = \sum_j H_{ij} P_{ij}(s) - \frac{1}{2} \langle x_i(s) \rangle, \quad (\text{A5})$$

where we have introduced the symmetric matrix

$$P_{ij}(s) = \frac{1}{N} \sum_\nu \frac{1}{k_\nu(k_\nu - 1)} \sum_{\substack{\lambda, \mu \in P_\nu \\ \mu \neq \lambda}} \langle n_{i,\lambda} n_{j,\mu} \rangle. \quad (\text{A6})$$

This matrix can be interpreted as the probability of sampling at time s a pair of individuals of species i and j when deciding

the replacement of a dead individual somewhere in the system. It satisfies $\sum_{ij} P_{ij}(s) = 1$ and, in a homogeneous network ($k_\nu = k, \forall \nu$), $\sum_{j=1}^g P_{ij}(s) = \langle x_i(s) \rangle$.

As for the second-order moments, both for $\mu \in P_\nu$ and for $\mu \notin P_\nu$, their equations read

$$\begin{aligned} \frac{d}{ds} \langle n_{i,\nu} n_{j,\mu} \rangle &= \frac{1}{k_\nu(k_\nu - 1)} \sum_l \sum_{\substack{\delta, \lambda \in P_\nu \\ \delta \neq \lambda}} H_{il} \langle n_{i,\lambda} n_{l,\delta} n_{j,\mu} \rangle \\ &+ \frac{1}{k_\mu(k_\mu - 1)} \sum_l \sum_{\substack{\delta, \lambda \in P_\nu \\ \delta \neq \lambda}} H_{jl} \langle n_{j,\lambda} n_{l,\delta} n_{i,\nu} \rangle \\ &- \langle n_{i,\nu} n_{j,\mu} \rangle. \end{aligned} \quad (\text{A7})$$

In general, it can be seen that the moment equations form a hierarchy, namely that the equation for a moment of order o depends on the moments of order $o + 1$. Hence, they cannot be solved in closed form, except if introducing some approximation.

2. Homogeneous mean-field approximation

The simplest of such approximations is the mean-field approach. It is conveniently done in the simplified case in which the network is spatially homogeneous, i.e. all the nodes have the same degree: $k_\nu = k, \forall \nu$. In this situation, we can search for statistically homogeneous solutions: $\langle n_{i,\nu}(s) \rangle = \rho_i(s), \forall \nu$. We can relate these time-dependent moments $\rho_i(s)$ to the macroscopic variables $x_i(s) \equiv N^{-1} \sum_\nu n_{i,\nu}(s)$ (note that $\sum_{i=1}^g x_i(s) = 1$). Indeed we have $\langle x_i \rangle = N^{-1} \sum_\nu \rho_i = \rho_i$, or $\langle x_i \rangle = \langle n_{i,\nu} \rangle$.

The mean-field approximation, which is exact in the case of all-to-all interactions in an infinite system, and expected to be accurate both for large enough interaction range (mean degree) and for unstructured interactions, consists in neglecting fluctuations and correlations:

$$\langle n_{i,\nu} \rangle = \langle x_i \rangle \simeq x_i, \quad \forall \nu \in \Sigma, \quad (\text{A8})$$

$$\langle n_{i,\nu} n_{j,\mu} \rangle \simeq \langle n_{i,\nu} \rangle \langle n_{j,\mu} \rangle \simeq x_i x_j, \quad \forall \nu \neq \mu \in \Sigma. \quad (\text{A9})$$

We have also $P_{ij} \approx x_i x_j$. Introduction of these expressions into Eq. (A4) leads to a closed evolution equation for x_i :

$$\frac{d}{ds} x_i = \left(\sum_l H_{il} x_l - \frac{1}{2} \right) x_i. \quad (\text{A10})$$

This mean-field equation has been studied before (e.g. [10]). We summarize here the main results:

First, the dynamics (A10) maintains in time the property $\sum_i x_i = 1$, if the initial condition satisfies it. This can be seen by defining $X \equiv \sum_i x_i$, calculating dX/ds , using that $H_{ij} = (H_{ij} + H_{ji})/2 = (1 - H_{ji} + H_{ij})/2$, and noticing that $\sum_{ij} (H_{ij} - H_{ji}) x_i x_j = 0$ and $\sum_{ij} x_i x_j = X^2$. Thus the sum of relative abundances satisfies

$$\frac{dX}{ds} = \frac{1}{2}(X^2 - X), \quad (\text{A11})$$

which maintains $X(t) = 1, \forall t$ if $X(0) = 1$.

Second, Eq. (A10) has several equilibria or fixed points. Many of them are of the ‘absorbing’ or ‘boundary’ type, i.e. steady solutions of (A10) in which $x_i = 0$ for some i , so that the corresponding species are extinct. In addition, if g is odd, there is generically [10] an *interior* equilibrium, $x_i(t) = x_i^*, \forall t$, in which all species coexist with non-vanishing relative abundances x_i^* . At this fixed point the relative abundances are given by

$$\sum_{j=1}^g H_{ij} x_j^* = \frac{1}{2} \Rightarrow x_i^* = \frac{1}{2} \sum_j (H^{-1})_{ij}, \quad (\text{A12})$$

where H^{-1} is the inverse of the dominance matrix, which always exists when it describes an intransitive loop. The properties of the boundary fixed points can be analyzed by recognizing that they can be considered interior equilibria in a system with a smaller number g of species.

Third, the dynamics from arbitrary initial conditions in which all x_i are non-vanishing (and for generic H) leads to a transient in which some of the species may become extinct. The remaining ones, an odd number, cycle neutrally around the interior fixed point (A12) in which the rows and columns corresponding to the extinct species have been removed from H [10]. The stability of this interior equilibrium is always neutral: relative abundances of surviving species describe periodic closed orbits around it, with an amplitude and period that is determined by the initial condition and without being attracted nor repelled by the fixed point. This can be seen [10] by noticing that the quantity

$$V(x_1, \dots, x_g) = - \sum_{i=1}^g x_i^* \log \frac{x_i}{x_i^*} \quad (\text{A13})$$

is a constant of motion, and thus it foliates the $(g-1)$ -simplex on which the dynamics occurs into invariant hypersurfaces that turn out to contain concentric closed orbits around the interior equilibrium.

The neutral character of the oscillations is not realistic from the biological point of view, and structurally unstable from the mathematical point of view. It is a consequence of the mean field approximation, and we expect such neutral cycling to be broken under corrections to mean-field, or under the full dynamics with finite range of interaction. This is indeed what is seen in our numerical simulations for the full model with three species: either the fixed point becomes attracting, or the neutral cycles are replaced by a single attracting limit cycle, with amplitude and period independent of the initial conditions.

In addition to its non-robust prediction of neutral cycling of the species, the mean-field approximation is not able to explain our main numerical finding: that the fixed point becomes stable for short-range interactions. From the observations of Sect. III C and Figure 4 it is likely that the stabilization of the fixed point arises from the fact that the relative abundances x_i are macroscopic quantities that become averaged and non-fluctuating when the microscopic structure contains many different domains, as in Figure 4a. Thus, it is pertinent trying to extend the mean-field formalism to describe the microscopic spatially-dependent configurations, as done in the following section.

3. Local mean-field and spatial stability

In this section we consider the species locations to be at the nodes of a two-dimensional square lattice. Then the node index ν can be considered to be a discrete two-dimensional vector. For regular networks such as this one, the mean-field

$$\frac{d}{ds}\rho_i(\nu, s) = \frac{1}{k(k-1)} \sum_j H_{ij} \left[\left(\sum_{\lambda \in P_\nu} \rho_i(\lambda, s) \right) \left(\sum_{\mu \in P_\nu} \rho_j(\mu, s) \right) - \sum_{\lambda \in P_\nu} \rho_i(\lambda, s) \rho_j(\lambda, s) \right] - \frac{1}{2} \rho_i(\nu, s). \quad (\text{A14})$$

We have used the notation $\langle n_{i,\nu} \rangle \equiv \rho_i(\nu, s)$. Note that this equation reduces to Eq. (A10) when ρ_i is homogeneous: $\rho_i(\nu, s) = x_i(s), \forall \nu$.

This new formulation allows us to assess the stability of particular solutions against spatially-dependent perturbations. For example we can focus on the stability of an homogeneous

approximation can be made local in space. This involves removing correlations as $\langle n_{i,\nu} n_{i,\nu} \rangle \simeq \langle n_{i,\nu} \rangle \langle n_{i,\nu} \rangle$ while keeping the dependence of the mean quantities on the node location.

Under this approximation, Eq. (A4) can be written as:

but time-dependent solution $\rho_i(\nu, s) = x_i(s)$ which verifies Eq. (A10). To do so, we seek a solution to Eq. (A14) of the form

$$\rho_i(\nu, s) = x_i(s) + \delta_i(\nu, s), \quad (\text{A15})$$

and linearize to first order in δ . With this, Eq. (A14) becomes

$$\frac{d\delta_i(\nu, s)}{ds} = \sum_j \frac{H_{ij}}{k} \left[x_j(s) \sum_{\lambda \in P_\nu} \delta_i(\lambda, s) + x_i(s) \sum_{\lambda \in P_\nu} \delta_j(\lambda, s) \right] - \frac{1}{2} \delta_i(\nu, s). \quad (\text{A16})$$

We introduce the Fourier transform of the perturbation: $\hat{\delta}_i(q, s) = \sum_\nu e^{iq \cdot \nu} \delta_i(\nu, s)$, in terms of which Eq. (A16) reads:

$$\frac{d\hat{\delta}_i(q, s)}{ds} = \left[-1 + 2F(q) \sum_j H_{ij} x_j(s) \right] \hat{\delta}_i(q, s) + F(q) x_i(s) \sum_j H_{ij} \hat{\delta}_j(q, s). \quad (\text{A17})$$

We have introduced the quantity

$$F(q) \equiv \frac{1}{k} \sum_{\lambda \in P_0} e^{iq \cdot \lambda}, \quad (\text{A18})$$

which satisfies $F(q=0) = 1$, $|F(q)| \leq 1$, and $F(q) \rightarrow 0$ as $|q| \rightarrow \infty$. Note that this quantity contains information on the interaction range through the dependence on P_0 (i.e. through the set of neighbors of the origin).

The simplest case to analyze is the stability of the interior equilibrium point, i.e. $x_i(s) = x_i^*, \forall s$ as given by Eq. (A12). In this case Eq. (A17) is a linear system with constant coefficients, hence the stability depends on the eigenvalues of the matrix of coefficients $M_{ij} = F(q) x_i^* H_{ij} + [F(q) - 1] \delta_{ij}/2$. In fact, because of Eq. (A11), there is always an unstable eigenvalue $1/2$ for perturbations that bring the dynamics out of the simplex. Thus, it is convenient to restrict the dynamics to the simplex by using $\sum_{j=1}^g \delta_j = 0$, and then the matrix of

the coefficients of Eq. (A17) restricted to the first $g-1$ dimensions is $M_{ij} = F(q) x_i^* (H_{ij} - H_{ig}) + [F(q) - 1] \delta_{ij}/2$, $i, j = 1, \dots, g-1$.

For example, for $g=3$, the two eigenvalues of M restricted to the simplex can be explicitly calculated and read

$$\lambda_{\pm} = -\frac{1-F}{2} \pm i \frac{F}{2} \sqrt{\frac{(2H_{12}-1)(2H_{13}-1)(2H_{23}-1)}{1-2(H_{12}-H_{13}+H_{23})}}. \quad (\text{A19})$$

The argument of the square root is always positive when H presents intransitive dominance cycles. Hence

$$\text{Re}[\lambda_{\pm}] = -\frac{1-F(\mathbf{q})}{2} \leq 0 \quad (\text{A20})$$

and the equality holds if and only if $\mathbf{q} = \mathbf{0}$. This means that, within the mean-field approximation, the steady and homogeneous solution $\rho_i(\nu, s) = x_i^*$ is linearly stable against small spatial perturbations, except for homogeneous perturbations, in which stability is marginal (a fact that we already knew from the more general nonlinear arguments in Sect. A 2). Thus, the local mean-field dynamics of Eq. (A14) leads, for inhomogeneous initial conditions close to the interior fixed point, to a homogenization of the configuration, which then proceeds to cycle neutrally around the fixed point. This is confirmed by direct numerical simulation of Eq. (A14). These results hold for any value of the interaction range, contained in $F(q)$. Thus, this local mean-field theory is not able to explain the results from our stochastic model with structured

interactions. Namely, a transition from persistent inhomogeneous configurations at short interaction range, which produce a fully attracting fixed point for the macroscopic variable $x_i(s) = \sum_\nu \rho(\nu, s)$, to a situation with oscillatory dynamics that produces a repelling fixed point and limit-cycle oscillations for $x_i(s)$ at large interaction range.

Nevertheless, we can still use the local mean-field to gain further insight into the dynamics, for example by analyzing the stability with respect to inhomogeneous perturbations of a homogeneous periodic solution $x_i(s)$ of Eq. (A10). In this case the stability equation (A17) is a linear equation with periodic coefficients, which can be analyzed with Floquet theory. The solutions can be written as a linear combination of the functions [32]

$$f_i(s)e^{p_i s}, \quad i = 1, \dots, g-1, \quad (\text{A21})$$

where $f_i(s)$ are periodic (and hence bounded) functions of time, with the same period T as the functions $x_i(s)$, and p_i are the Floquet exponents given in terms of the eigenvalues Λ_i of the fundamental matrix $\Phi(s)$ of system (A17), satisfying $\Phi(0) = I$, as

$$\Lambda_i = e^{p_i T}. \quad (\text{A22})$$

When all p_i are negative, the perturbations decay and the homogeneous solution $x_i(s)$ is recovered as time advances. We have numerically evaluated p_i for the case of three species, $g = 3$, and some values of the parameters of the system. For all cases considered, p_i has always negative real parts (except for homogeneous perturbations, for which one finds neutral stability), meaning that any initial inhomogeneous perturbation tends to disappear. This agrees with direct simulation results of Eq. (A14). Thus, the long-term behavior of the local mean-field approach reduces to the standard homogeneous mean-field treatment of Sect. A 2. In contrast, simulation of the stochastic model shows domains of the different species for short interaction range.

However, the stability strength is not the same for all parameter values. Let $M(s)$ be the matrix of time-dependent coefficients of the system (A17). A necessary, but not sufficient, condition for the homogeneous solutions $x_i(s)$ to be unstable is that some eigenvalue of $M(s)$ has positive real part for some time $s \in [0, T]$ (see a proof of a similar result in [31]). During these times, even if the trajectory turns out to be linearly stable, its stability is reduced and more susceptible to non-infinitesimal perturbations or noise. For the case of three species $g = 3$, and the interaction matrix H given again by Eq. (1), we have seen that the matrix $M(s)$ has eigenvalues with positive real parts, for some possible periodic trajectories $x_i(s)$, provided $F(q) \gtrsim 0.67$. Since the maximum of $F(q)$ occurs at zero wavenumber and the width of this function decreases with increasing k , the band of wavenumber identified as ‘less-stable’ shrinks as the interaction range, quantified by k increases. This is an indication (although not a proof) that homogeneous periodic solutions would be more robust for long-range interactions, and instabilities giving rise to inhomogeneous configurations are more likely to occur for short-range interactions. It is interesting to note that the times at

which the matrix $M(s)$ has more positive real-part of eigenvalues coincide with the times at which some of the components of the oscillatory solution $x_i(s)$ approach zero.

On general grounds, the local mean-field approximation should represent some kind of coarse-graining of the original stochastic system, and should be completed by noise terms to gain accuracy. Under short-range interactions, appropriate noise terms would be able to break the synchronization between distant locations, and reproduce the domain structure observed in the Monte Carlo simulations. However, we find difficult to write analytical expressions for these noise terms that would respect all the proper statistical constraints (for example: reflect the multiplicative nature of birth-death fluctuations, keep in time that $\sum_i \rho_i(\nu, s) = 1$, etc.). Also, the complexity of such model would not be lower than the original individual-based one. Thus, we have not developed further this possibility.

Appendix B: Effect of introducing correlations beyond mean-field

In section III C we demonstrated that short-range interactions lead to the emergence of mono-specific clusters, effectively increasing intra-specific competition and stabilizing the dynamics. As a further way to confirm that the decline of inter-specific competition is able to change the stability of the equilibrium, making it stable for sufficiently reduced competition between distinct species, we have studied a toy-model which shares characteristics with our community model. It is built by noticing that $\langle P_{ij} \rangle$ is just the time average of the matrix $P_{ij}(s)$ in Eq. (A6) of Appendix A. A way to correct the mean-field approximation $P_{ij} \approx x_i x_j$ is to introduce some correlations, $P_{ij} \approx c_{ij} x_i x_j$, making some ansatz for c_{ij} and introducing it into the exact equation (A5) (with $\langle x_i \rangle \approx x_i$). We have explored the behavior of such model in which correlations are implemented by $c_{ij} = 1 - \epsilon$ if $i \neq j$ and $c_{ii} = 1 + \epsilon'$, with $\epsilon, \epsilon' > 0$, resulting in an enhanced intra-specific competition with respect to inter-specific competition as ϵ and ϵ' are increased. With this choice of c_{ij} the resulting matrix P_{ij} does not have the proper statistical properties. In particular the model does not respect that $\sum_i x_i = 1, \forall s$. However, this problem can be fixed by constraining the dynamics onto the simplex by subtracting to Eq. (A5), for each species i , the same term $g^{-1} \sum_i G_i$, where G_i is the right-hand-side of Eq. (A5). It should be clear that this is not a systematic approximation to our original system, but a toy model useful to check the impact of varying the intra- and inter-specific competition balance. For example, for $\epsilon' = 0.01$ and the same dominance matrix used in the rest of the paper, we have found that a Hopf bifurcation occurs at $\epsilon = \epsilon_c \approx 0.01975$, so that relative species abundances undergo limit cycle oscillations for $\epsilon < \epsilon_c$ but the fixed point becomes stable and attracting when the inter-specific competition is further reduced, $\epsilon > \epsilon_c$. These are the same type of states and the same transition that is encountered in our stochastic model when decreasing the interaction range.

-
- [1] R. M. May, Will a large complex system be stable?, *Nature* **238**, 413 (1972).
- [2] P. Chesson, Updates on mechanisms of maintenance of species diversity, *Journal of Ecology* **106**, 1773 (2018).
- [3] S. Allesina and S. Tang, The stability-complexity relationship at age 40: a random matrix perspective, *Population Ecology* **57**, 63 (2015).
- [4] G. Bunin, Ecological communities with Lotka-Volterra dynamics, *Phys. Rev. E* **95**, 042414 (2017).
- [5] L. Sidhom and T. Galla, Ecological communities from random generalized Lotka-Volterra dynamics with nonlinear feedback, *Phys. Rev. E* **101**, 032101 (2020).
- [6] I. Bartomeus and O. Godoy, Biotic controls of plant coexistence, *Journal of Ecology* **106**, 1767 (2018).
- [7] R. M. May and W. J. Leonard, Nonlinear Aspects of Competition Between Three Species, *SIAM Journal on Applied Mathematics* **29**, 243 (1975).
- [8] R. A. Laird and B. S. Schamp, Species coexistence, intransitivity, and topological variation in competitive tournaments, *Journal of Theoretical Biology* **256**, 90 (2009).
- [9] B. Kerr, M. A. Riley, M. W. Feldman, and B. J. Bohannan, Local dispersal promotes biodiversity in a real-life game of rock-paper-scissors, *Nature* **418**, 171 (2002).
- [10] J. Grilli, G. Barabás, M. J. Michalska-Smith, and S. Allesina, Higher-order interactions stabilize dynamics in competitive network models, *Nature* **548**, 210 (2017).
- [11] G. Losapio, A. Montesinos-Navarro, and H. Saiz, Perspectives for ecological networks in plant ecology, *Plant Ecology & Diversity* **12**, 87 (2019).
- [12] J. M. Levine, J. Bascompte, P. B. Adler, and S. Allesina, Beyond pairwise mechanisms of species coexistence in complex communities, *Nature* **546**, 56 (2017).
- [13] F. Battiston, E. Amico, A. Barrat, G. Bianconi, G. Ferraz de Arruda, B. Franceschiello, I. Iacopini, S. Kéfi, V. Latora, Y. Moreno, *et al.*, The physics of higher-order interactions in complex systems, *Nature Physics* **17**, 1093 (2021).
- [14] G. Hardin, The competitive exclusion principle, *Science* **131**, 1292 (1960).
- [15] F. Valladares, C. C. Bastias, O. Godoy, E. Granda, and A. Escudero, Species coexistence in a changing world, *Frontiers in Plant Science* **6**, 866 (2015).
- [16] U. Dieckmann, R. Law, and J. A. J. Metz, eds., *The Geometry of Ecological Interactions* (Cambridge University Press, Cambridge, 2000).
- [17] N. V. Lowery and T. Ursell, Structured environments fundamentally alter dynamics and stability of ecological communities, *Proceedings of the National Academy of Sciences of the United States of America* **116**, 379 (2019).
- [18] J. Travis, R. Brooker, and C. Dytham, The interplay of positive and negative species interactions across an environmental gradient: insights from an individual-based simulation model, *Biology Letters* **1**, 5 (2005).
- [19] M. Pascual, M. Roy, F. Guichard, and G. Flierl, Cluster size distributions: Signatures of self-organization in spatial ecologies, *Philosophical Transactions of the Royal Society B: Biological Sciences* **357**, 657 (2002).
- [20] S. Kéfi, M. Rietkerk, C. L. Alados, Y. Pueyo, V. P. Papanastasis, A. ElAich, and P. C. De Ruiter, Spatial vegetation patterns and imminent desertification in Mediterranean arid ecosystems, *Nature* **449**, 213 (2007).
- [21] J. Liao, J. Chen, Z. Ying, D. E. Hiebeler, and I. Nijs, An extended patch-dynamic framework for food chains in fragmented landscapes, *Scientific Reports* **6**, 1 (2016).
- [22] J. Chave, H. C. M. Landau, and S. A. Levin, Comparing classical community models: Theoretical consequences for patterns of diversity, *The American Naturalist* **159**, 1 (2013).
- [23] S. Allesina, J. Grilli, G. Barabás, S. Tang, J. Aljadeff, and A. Maritan, Predicting the stability of large structured food webs, *Nature Communications* **6**, 7842 (2015).
- [24] J. Dall and M. Christensen, Random geometric graphs, *Phys. Rev. E* **66**, 016121 (2002).
- [25] P. Erdős and A. Rényi, On random graphs, *Publ. Math. Debrecen* **6**, 290 (1959).
- [26] V. Grimm and S. Railsback, *Individual-based Modeling and Ecology* (Princeton University Press, 2005).
- [27] A. Cardillo, S. Meloni, J. Gómez-Gardeñes, and Y. Moreno, Velocity-enhanced cooperation of moving agents playing public goods games, *Phys. Rev. E* **85**, 067101 (2012).
- [28] E. Estrada, S. Meloni, M. Sheerin, and Y. Moreno, Epidemic spreading in random rectangular networks, *Physical Review E* **94**, 052316 (2016).
- [29] J. H. Arias, J. Gómez-Gardeñes, S. Meloni, and E. Estrada, Epidemics on plants: Modeling long-range dispersal on spatially embedded networks, *Journal of Theoretical Biology* **453**, 1 (2018).
- [30] N. Khalil, C. López, and E. Hernández-García, Nonlocal birth-death competitive dynamics with volume exclusion, *Journal of Statistical Mechanics: Theory and Experiment* **2017**, 063505 (2017).
- [31] K. Klemm and N. Khalil, Altruism in populations at the extinction transition, *Physical Review Research* **2**, 013374 (2020).
- [32] P. Glendinning, *Stability, instability and chaos: an introduction to the theory of nonlinear differential equations*, Vol. 11 (Cambridge University Press, 1994).